Original Article

Munc13-1 Deficiency Reduces Insulin Secretion and Causes Abnormal Glucose Tolerance

Edwin P. Kwan,[1] Li Xie,[2] Laura Sheu,[2] Christopher J. Nolan,[3] Marc Prentki,[3] Andrea Betz,[4] Nils Brose,[4] and Herbert Y. Gaisano[1,2]

Munc13-1 is a diacylglycerol (DAG) receptor that is essential for synaptic vesicle priming. We recently showed that Munc13-1 is expressed in rodent and human islet β-cells and that its levels are reduced in islets of type 2 diabetic humans and rat models, suggesting that Munc13-1 deficiency contributes to the abnormal insulin secretion in diabetes. To unequivocally demonstrate the role of Munc13-1 in insulin secretion, we studied heterozygous Munc13-1 knockout mice (+/−), which exhibited elevated glucose levels during intraperitoneal glucose tolerance tests with corresponding lower serum insulin levels. Munc13-1$^{+/-}$ mice exhibited normal insulin tolerance, indicating that a primary islet β-cell secretory defect is the major cause of their hyperglycemia. Consistently, glucose-stimulated insulin secretion was reduced 50% in isolated Munc13-1$^{+/-}$ islets and was only partially rescued by phorbol ester potentiation. The corresponding alterations were minor in mice expressing one allele of a Munc13-1 mutant variant, which does not bind DAG (H567K/+). Capacitance measurements of Munc13-1$^{+/-}$ and Munc13-1$^{H567k/+}$ islet β-cells revealed defects in granule priming, including the initial size and refilling of the releasable pools, which become accentuated by phorbol ester potentiation. We conclude that Munc13-1 plays an important role in glucose-stimulated insulin secretion and that Munc13-1 deficiency in the pancreatic islets as occurs in diabetes can reduce insulin secretion sufficient to cause abnormal glucose homeostasis. *Diabetes* 55:1421–1429, 2006

From the [1]Department of Physiology, University of Toronto, Toronto, Ontario, Canada; the [2]Department of Medicine, University of Toronto, Toronto, Ontario, Canada; the [3]Molecular Nutrition Unit, Department of Nutrition, University of Montreal, the Centre Hospitalier de l'Universite de Montreal and the Montreal Diabetes Research Center, Montreal, Quebec, Canada; and the [4]Department of Molecular Neurobiology, Max Planck Institute of Experimental Medicine, Göttingen, Germany.

Address correspondence and reprint requests to Dr. Herbert Gaisano, Medical Sciences Bldg., Rm. 7226, 1 King's College Circle, University of Toronto, Toronto, Ontario M5S 1A8, Canada. E-mail: herbert.gaisano@utoronto.ca.

Received for publication 27 September 2005 and accepted in revised form 8 February 2006.

C_m, membrane capacitance; DAG, diacylglycerol; GSIS, glucose-stimulated insulin secretion; IPGTT, intraperitoneal glucose tolerance test; KRBH, Krebs-Ringer bicarbonate buffer containing 10 mmol/l HEPES; PKC, protein kinase C; PMA, phorbol 12-myristate 13-acetate ester; RRP, readily releasable pool; SNARE, soluble *N*-ethylmaleimide–sensitive factor attachment protein receptor.

DOI: 10.2337/db05-1263

Normal glucose-stimulated insulin secretion (GSIS) from pancreatic islets follows a biphasic pattern (1). The first phase is a robust release lasting ~5–10 min and is triggered by ATP-sensitive K^+ channel–dependent Ca^{2+} entry into the pancreatic β-cells. This is followed by a second phase and sustained release, which is regulated by second messengers including diacyglycerol (DAG), cAMP, and permissive elevated levels of Ca^{2+} (2). In patients with type 2 diabetes, this pattern of secretion is perturbed, resulting in an abolished first phase and a blunted second phase (2). It is generally accepted that the biphasic secretion pattern is contributed by the release of spatially and functionally distinct insulin granules. The morphologically docked granule pool at the plasma membrane contains <10% of the total of >10,000 insulin granules per cell, and only a fraction (20–30%) of the docked pool is primed and fusion competent for immediate release (3). It is the release of this docked and primed granule pool that contributes to the first phase of insulin secretion (2–4). One of the aims of the present study was to identify the proteins that prime insulin granules for release.

As in neurons (5), exocytosis in pancreatic islet β-cells is regulated by the SNARE (soluble *N*-ethylmaleimide–sensitive factor attachment protein [SNAP] receptor) proteins VAMP, SNAP-25, and syntaxin-1A (6). These SNARE proteins form a ternary complex capable of driving the vesicular fusion reaction (7). SNARE protein functions in mammals are regulated by Munc13 proteins (8), which constitute a family of three largely brain-specific homologues of *Caenorhabditis elegans* Unc-13 (9) and *Drosophila* Dunc-13 (10) and Munc13-1, -2, and -3 (11,12). Genetic deletion studies in mice, *C. elegans* and *Drosophila* showed that Munc13s/Unc-13/Dunc-13 are essential secretory vesicle priming proteins, whose absence leads to complete loss of fusion-competent synaptic vesicles (10,13–15). At the molecular level, Unc-13/Munc13-1 is generally thought to mediate vesicle priming by unfolding or activating syntaxin and thereby promoting SNARE complex formation (8,16). Whereas the worm's (14) and fly's (10) Munc13 homologues are each encoded by a single gene, mammalian Munc13-1, -2, and -3 are encoded by three separate genes (12) that exhibit both overlapping as well as distinct tissue- and subcellular distributions (11,12,17). These Munc13 isoforms belong to the superfamily of C_2 domain proteins and Munc13s 1-3 contain a DAG-binding C_1 domain (8,9,12,18). The Munc13 C_1 domain acts as the main presynaptic targets of DAG, and binding of DAG or phorbol esters leads to their membrane

translocation (18) and enhances the priming activity of Munc13 proteins (18,19). This, in turn, increases the size of the readily releasable vesicle pool (RRP) size and synaptic release probability (19).

We recently reported that the levels of Munc13-1 are severely reduced in pancreatic islets of type 2 diabetic GK and *fa/fa* Zucker rats (20) as well as in diabetic human islets (21). Islet levels of syntaxin 1A and the nSec1/Munc18-1 proteins are also reduced. Overexpression of Munc13-1 in insulinoma cells greatly potentiated insulin exocytosis evoked by glucose and phorbol-ester stimulation (20). This led us to postulate that reduced levels of Munc13-1 and SNARE proteins may directly contribute to the dysregulated insulin release from diabetic islets. To directly test the specific role of Munc13-1 in insulin secretion, we have examined glucose homeostasis and insulin secretion in genetically modified mice deficient in either Munc13-1 expression or function. Using Munc13-1–deficient mice (Munc13-$1^{-/-}$) and knockin mice (Munc13-$1^{H567K/H567K}$), the latter carrying a single-point mutation (H567K) within the Munc13-1 C_1 domain that abolishes DAG and phorbol ester binding, we showed previously that Munc13 proteins are the primary presynaptic phorbol ester receptors and mediate the priming of synaptic vesicles (19,22). Since mice homozygous for either one of these mutations die shortly after birth, we have used in the present study heterozygous mice (Munc13-$1^{+/-}$ and Munc13-$1^{H567K/+}$) to examine the islet Munc13-1 actions in insulin secretory granule priming, assuming that the reduced islet levels of Munc13-1 in heterozygous deletion mutant mice would mimic the Munc13-1 deficiency observed in type 2 diabetes (20,21). We show that heterozygous Munc13-1–deficient (Munc13-$1^{+/-}$) mice exhibit glucose intolerance that is caused by impaired insulin secretion. This provides direct support for the view that Munc13-1 is a key signaling protein implicated in the coupling mechanisms of insulin exocytosis.

RESEARCH DESIGN AND METHODS

Munc13-$1^{+/-}$ knockout and Munc13-$1^{H567K/+}$ knockin mice were described previously (13,19). The genotypes of the mice were determined by PCR and DNA electrophoresis as described (13,19). Mice were housed on a 12-h light/dark cycle and were allowed free access to standard mouse food and water. All experimental procedures have been approved by the Animal Care Committee of the University of Toronto.

Glucose and insulin tolerance tests. Glucose (1 g/kg body wt) tolerance tests were performed about bimonthly on 12- to 32-week-old Munc13-$1^{+/+}$, Munc13-$1^{+/-}$, and Munc13-$1^{H567K/+}$ mice after a 12- to 16-h fasting period by intraperitoneal injection. The purpose of using older mice of up to 32 weeks of age was to assess a possible recovery from or worsening of glucose intolerance in Munc13-$1^{+/-}$ and Munc13-$1^{H567K/+}$ mice. Within each group, there was no change in glucose tolerance over the period, and the data were therefore pooled. Blood samples were obtained from the tail vein at the times indicated following glucose injection. Blood glucose concentrations were measured with a Lifescan OneTouch basic glucose meter (Lifescan Canada, Burnaby, Canada). During the glucose tolerance test (above), blood samples were also obtained from the legs' saphenous vein at the times indicated after the glucose load. Serum was separated from plasma by centrifugation and stored at −20°C until serum insulin concentrations were determined using a radioimmunoassay kit (Linco Research, St. Louis, MO). For the insulin tolerance test, human biosynthetic insulin (Novo Nordisk, Toronto, Canada) was injected intraperitoneally at a dose of 0.55 units/kg body wt into mice after a 5-h fasting period. A drop of blood was withdrawn from the tail vein at the indicated times following insulin administration.

Isolation of mouse pancreatic islets and isolated β-cells. Mice were sacrificed by cervical dislocation. The abdominal cavity was opened, the pancreatic duct cannulated under a dissecting microscope, and 2 ml of a collagenase solution (2 mg/ml; Worthington Biochemical, Lakewood, NJ) dissolved in Hanks' balanced salt solution containing 10 mmol/l HEPES (pH 7.4) was injected, which dilates the pancreas. Pancreas was then excised and incubated in the same solution at 37°C for 26 min with shaking to disrupt the tissue. Pancreatic tissues were then filtered through a nylon gauze and washed extensively with collagenase-free Hanks' balanced salt solution/HEPES. The islets were then hand picked under an upright stereomicroscope and maintained in culture medium. Dispersed single β-cells were obtained by incubating islets in Ca^{2+}/Mg^{2+}-free PBS containing 5 mmol/l EDTA and 0.25 mg/ml trypsin for 10 min at 37°C with mild shaking. Isolated cells were cultured in RPMI 1640 medium containing 11 mmol/l glucose supplemented with 10% FCS, 100 units/ml penicillin, 100 μg/ml streptomycin, 10 mmol/l HEPES (pH 7.4), and 1 mmol/l sodium pyruvate at 37°C in a humidified atmosphere containing 5% CO_2. β-Cells were allowed to adhere on coverslips for ~48 h before electrophysiological experiments. β-Cells were cultured for up to 4 days, but the majority of the electrophysiological studies were performed at 2–4 days.

Immunoblotting. Isolated islets were solubilized in sample buffer (with 2% SDS), and the indicated amount of protein of each sample was loaded and separated on SDS polyacrylamide gels (Munc13-1, 15 μg of protein/lane, 6% PAGE; nsec1/Munc18-1, syntaxin 1A, 5 μg of protein/lane, 14% PAGE; protein kinase C [PKC]-α and -ε, 18 μg of protein/lane, 7.5% PAGE). Separated proteins were transferred to nitrocellulose membranes and incubated with the following rabbit polyclonal primary antibodies for 1.5–2 h at room temperature: anti-Munc13-1, 1:5,000 (19); anti-syntaxin 1A, 1:1,000 (Calbiochem, San Diego, CA); anti-nsec1/Munc18-1, 1:1,000 (Transduction Laboratories, Lexington, KY); anti-PKC-α, 1:1,000 (Sigma); and anti-PKC-ε, 1:1,000 (Sigma). Primary antibodies were detected with peroxidase-labeled goat anti-rabbit secondary antibodies. Positive reactions were visualized by chemiluminescence (Pierce) and exposure of the membranes to Kodak BMR film (Eastman Kodak, Rochester, NY) for 1 s to 10 min.

Islet insulin secretion and insulin content measurements. To allow freshly isolated islets to recover after isolation, islets from Munc13-$1^{+/+}$, Munc13-$1^{+/-}$, and Munc13-$1^{H567K/+}$ mice at ages 4–8 months were cultured for 2 h as described above in medium containing 11 mmol/l glucose. The islets were then cultured for 2 h in the same conditions except that the medium contained 2.8 mmol/l glucose. Afterward, the similar-size islets were picked and distributed in batches of ~30 into 12-well plates, with four replicates for each condition per genotype. They were then washed and preincubated for 40 min at 37°C in 1 ml Krebs-Ringer bicarbonate buffer containing 10 mmol/l HEPES (KRBH; pH 7.4), 0.5% BSA, and 3 mmol/l glucose. The islets were then incubated for 1 h at 37°C in 1 ml of KRBH containing 3 mmol/l glucose, followed by 1 h at 37°C in 1 ml of KRBH containing 16 mmol/l glucose in the absence or presence of 200 nmol/l phorbol 12-myristate 13-acetate ester (PMA) (Sigma). At the end of each 1-h incubation, media were collected for insulin determination. Total insulin content of the islets was measured after acid-ethanol (0.2 mmol/l HCl in 75% ethanol) extraction. Insulin was measured by radioimmunoassay, as described above, and insulin secreted into the supernatant was expressed as percentage of total islet insulin content per hour to ensure accuracy and reduce intra- and interassay variation.

Electrophysiology. Patch electrodes were pulled from 1.5-mm thin-walled borosilicate glass and polished to a tip resistance of 2–4 MΩ when filled with intracellular solution. β-Cells were identified by the lack of a transient voltage-dependent inward Na^+ current as described by Gopel et al. (23). For capacitance measurements, the patch electrodes were coated with orthodontic wax (Butler, Guelph, Canada) close to the tips and fire polished. The pipette solution contained (in mmol/l): 125 K-glutamate, 10 KCl, 10 NaCl, 1 $MgCl_2$, 5 HEPES, 0.05 EGTA, and 4 MgATP, pH to 7.1. The extracellular solutions consisted of (in mmol/l): 138 NaCl, 5.6 KCl, 1.2 $MgCl_2$, 2.6 $CaCl_2$, 5 HEPES, and 5 D-glucose, pH to 7.4. For the measurements with PMA stimulations, the β-cells were preincubated with 200 nmol/l PMA for ~10 min, and this concentration was maintained in the incubation chamber during recordings. Cell capacitance was determined by the Lindau-Neher technique (24), implementing the "Sine + DC" feature of the Lock-in module (40 mV peak-to-peak and a frequency of 500 Hz) in the standard whole-cell mode. Recordings were conducted using an EPC-10 patch clamp amplifier and Pulse software (HEKA Electronics, Lambrecht/Pflaz, Germany). Exocytotic events were elicited by a train of eight 500-ms depolarizing pulses (1-Hz stimulation frequency) from −70 to 0 mV. All capacitance measurements were performed at 30°C.

For the measurement of Ca_V currents, pipettes were filled with (in mmol/l): 120 CsCl, 20 tetraethylammonium chloride, 5 EGTA, 5 MgATP, and 5 HEPES (pH 7.2). The external solution was comprised of (in mmol/l): 100 NaCl, 20 $BaCl_2$, 20 tetraethylammonium, 4 CsCl, 1 $MgCl_2$, 10 glucose, and 5 HEPES (pH 7.4). Tetraethylammonium was used to block K_V currents. For K_V current measurements, pipettes were filled with (in mmol/l): 125 K-glutamate, 10 KCl, 10 NaCl, 1 $MgCl_2$, 5 HEPES, 0.05 EGTA, and 4 MgATP, pH to 7.1. The extracellular solutions consisted of (in mmol/l): 138 NaCl, 5.6 KCl, 1.2 $MgCl_2$, 2.6 $CaCl_2$, 5 HEPES, and 5 D-glucose, pH to 7.4. To elicit K_V and Ca_V currents, cells were held at −80 mV and depolarized from −80 to +80 mV in 10-mV

increments using 500-ms step pulses and from −60 to +80 mV in 10-mV increments using 200-ms step pulses, respectively. Steady-state inactivation properties of Ca_V currents were investigated by depolarizing the cells with 1-s prepulse from −100 to 60 mV. Steady-state inactivation curves were fit with a Boltzmann equation: I/Imax = 1/(1 + exp[V-V1/2]/k), where V1/2 is the voltage at which half of the channels are inactivated, and k is the slope factor. All Ca_V and K_V currents recordings were performed at room temperature.

Statistical analysis. Where appropriate, results are expressed as means ± SE. Statistical analysis was performed by unpaired Student's *t* test or repeated measure ANOVA, where $P < 0.05$ was considered significant.

RESULTS

Munc13-1 levels are reduced in Munc13-1$^{+/-}$ mouse pancreatic islet. Homozygous Munc13-1$^{-/-}$ and Munc13-1$^{H567K/H567K}$ mice exhibit severely impaired neurotransmitter release and die shortly after birth (13,19). We have therefore used heterozygous mice (+/− and ^{H567K}/+) to examine the effects of Munc13-1 deficiency on glucose homeostasis and insulin secretion. The heterozygous mice do not exhibit neurological deficits (13,19). The expression levels of Munc13-1 in Munc13-1$^{+/+}$, Munc13–1$^{+/-}$, and Munc13-1$^{H567K/+}$ mouse brains were determined by Western blotting using a rabbit antibody generated against the NH_2-terminal amino acids 1–305 of Munc13-1 (19,20). Consistent with previous reports (19), Munc13-1 levels were significantly reduced by 20% ($n = 2$) in the brains of Munc13-1$^{+/-}$ mice compared with wild-type Munc13-1$^{+/+}$ control mice (Fig. 1*A*). Brain Munc13-1 levels were similar in Munc13-1$^{H567K/+}$ mice and wild-type controls, since the H567K mutant protein is of the same size as the native Munc13-1 protein (19). Brain levels of syntaxin 1A and nSec1/Munc18-1 were identical in the three groups of mice. Islet tissue levels of Munc13-1 were reduced by 60% ($n = 4$) in Munc13-1$^{+/-}$ mice as compared with wild-type islets, whereas those of Munc13-1$^{H567K/+}$ was 97% of those of Munc13-1$^{+/+}$ islet levels (Fig. 1*B*). The levels of syntaxin 1A, nSec1, and PKC-α and -ε in the islets of Munc13-1$^{+/-}$ and Munc13-1$^{H567K/+}$ mice were similar to those of wild-type Munc13-1$^{+/+}$ islets. The results indicate that possible defects of insulin secretion in the islet β-cells from the two types of heterozygous mutants would be attributed to the Munc13-1 deficiency per se and not to a deficiency in the expression of Munc13-1–interacting proteins or the other DAG-binding proteins, specifically the putative PKC isoforms reported to influence insulin secretion (25–27). In contrast, complete loss of Munc13-1 (−/−) induces a mild reduction in a number of the t-SNARE syntaxin and several associated proteins in the brain (13,19). A major reduction in the levels of SNARE proteins and nSec1 also accompanies Munc13-1 deficiency in the diabetic GK and Zucker rat islets as we have previously reported (20).

Munc13-1$^{+/-}$ mice exhibit abnormal glucose tolerance. Intraperitoneal glucose tolerance tests (IPGTTs) indicated that Munc13-1$^{+/-}$ mice displayed a glucose-intolerant phenotype (Fig. 2). Male Munc13-1$^{+/-}$ mice exhibited significantly ($P \leq 0.05$) higher glucose levels in response to a glucose load at $t = 15$ and 30 min. Fasting glucose levels were, however, not significantly different between Munc13-1$^{+/-}$ (6.8 ± 0.3 mmol/l) and wild-type Munc13-1$^{+/+}$ control (6.6 ± 0.2 mmol/l) mice. Munc13-1$^{H567K/+}$ mice also showed normal fasting glycemia (6.8 ± 0.2 mmol/l). Surprisingly, the Munc13-1$^{H567K/+}$ mice exhibited overall normal glucose tolerance, indicating that expression of the Munc13-1 mutant variant may not lead to sufficient insulin secretory deficiency to cause an abnormal glucose homeostasis, although glucose levels at $t =$ 20–30 min were slightly but not significantly elevated. We next investigated whether this abnormal glucose homeostasis is due to either a defect in insulin secretion or a defect in insulin sensitivity of the peripheral tissues. Following insulin injection, glucose levels were similarly lowered in the three groups, indicating no difference in insulin sensitivity (Fig. 3).

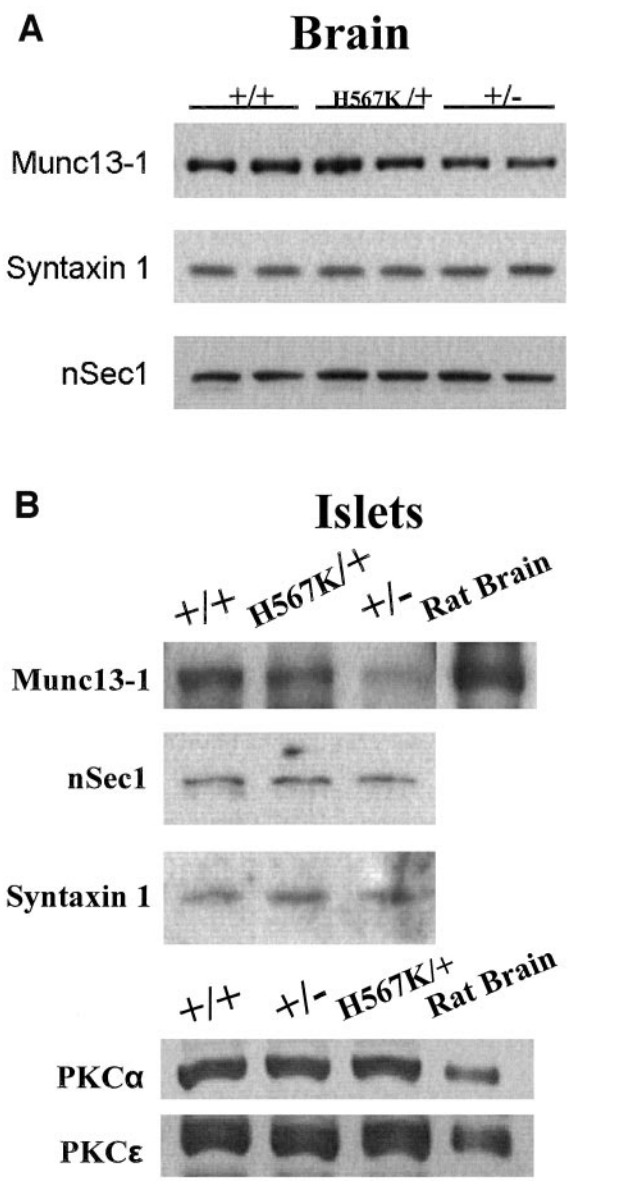

FIG. 1. Munc13-1 levels in brain and pancreatic islets of Munc13-1$^{+/+}$ vs. Munc13-1$^{+/-}$ and Munc13-1$^{H567K/+}$ mice. *A*: Western blots of Munc13-1, syntaxin 1, and nSec1/Munc18-1 proteins from the brains (paired samples) of Munc13-1$^{+/+}$, Munc13-1$^{+/-}$, and Munc13-1$^{H567K/+}$ mice. A total of 15 μg of protein/lane were loaded for Munc13-1 and 5 μg of protein/lane for each of nSec1/Munc18-1 and syntaxin 1A. *B*: Western blots of the above proteins and PKC-α and -ε from pancreatic islets. A total of 15 μg of protein/lane were loaded for Munc13-1 and 5 μg for each of nSec1/Munc18-1 and syntaxin 1A and 18 μg for each of PKC-α and -ε. This is representative of two to four separate experiments. Note that Munc13-1 levels were reduced in heterozygous Munc13-1$^{+/-}$ islets, whereas the heterozygous H567K mutation in the C1 domain does not alter the expression of Munc13-1 proteins in the Munc13-1$^{H567K/+}$ islets. The expression levels of nSec1, syntaxin 1, and PKC-α and -ε are comparable between the Munc13-1$^{+/+}$, Munc13-1$^{+/-}$, and Munc13-1$^{H567K/+}$ islets.

Munc13-1$^{+/-}$ mice exhibit reduced insulin secretion in vivo. Munc13-1$^{+/-}$ mice showed similar fasting serum insulin levels (0.41 ± 0.04 ng/ml) as those of Munc13-1$^{+/+}$

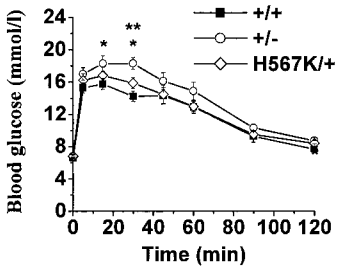

FIG. 2. Glucose tolerance is abnormal in Munc13-1$^{+/-}$ mice and normal in Munc13-1$^{H567K/+}$ mice. Intraperitoneal glucose (1 g/kg body wt) tolerance tests were performed on 12- to 16-h–fasted Munc13-1$^{+/+}$, Munc13-1$^{+/-}$, and Munc13-1$^{H567K/+}$ mice and glucose levels measured as described under RESEARCH DESIGN AND METHODS. Values are means ± SE of ~10 animals per group. *P < 0.05 for Munc13-1$^{+/-}$ vs. Munc13-1$^{+/+}$ mice; **P < 0.05 for Munc13-1$^{+/-}$ vs. Munc13-1$^{H567K/+}$ mice.

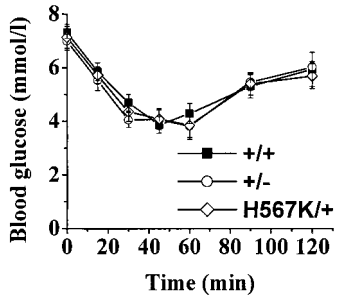

FIG. 3. Munc13-1$^{+/-}$ and Munc13-1$^{H567K/+}$ mice display normal insulin tolerance. Intraperitoneal insulin (0.55 units/kg body wt) tolerance tests were performed in 5-h–fasted Munc13-1$^{+/+}$, Munc13-1$^{+/-}$, and Munc13-1$^{H567K/+}$ mice and glucose levels measured as described under RESEARCH DESIGN AND METHODS. Data are means ± SE of ~6 mice per group.

mice (0.47 ± 0.05 ng/ml). However, in response to a glucose load during IPGTT, Munc13-1$^{+/-}$ mice consistently showed lower serum insulin levels with respect to Munc13-1$^{+/+}$ mice (Fig. 4*A*). The t = 10 min level, which corresponds to the first phase of insulin release, was lower in Munc13-1$^{+/-}$ (0.65 ± 0.07 ng/ml) compared with wild-type (0.95 ± 0.08 ng/ml) mice. Serum insulin levels at t = 30 min, which corresponds to the second phase of insulin release, was also lower in the Munc13-1$^{+/-}$ mice (0.52 ± 0.03 ng/ml) as compared with wild-type (0.73 ± 0.05 ng/ml) mice. A similar observation was made at t = 120 min. Insulin secretion as indirectly assessed as the area under the curve representing the time course of release over the entire 2-h period, encompassing first- and second-phase release, showed an ~50% reduction in Munc13-1$^{+/-}$ mice (Fig. 4*B*). As for the Munc13-1$^{H567K/+}$ mice, serum insulin levels were lower at t = 10 min (0.59 ± 0.15 ng/ml), but during the second phase of insulin release, insulin levels were similar at 30 and 120 min. The area under the curve in Munc13-1$^{H567K/+}$ mice showed no difference with respect to wild-type mice.

Glucose-stimulated insulin secretion is impaired in isolated islets from Munc13-1$^{+/-}$ mice. We then examined insulin secretion from freshly isolated pancreatic islets of the different Munc13-1 mutant mice (Fig. 5). There was no difference in basal (3 mmol/l glucose) insulin secretion between the groups. However, GSIS (16 mmol/l glucose-stimulated secretion above basal) was greatly reduced in Munc13-1$^{+/-}$ mice islets with respect to Munc13-1$^{+/+}$ mice islets. Relative to basal insulin release, Munc13-1$^{+/-}$ islet GSIS was 1.68-fold basal release, which is a reduction of 52% with respect to Munc13-1$^{+/+}$ mice islets (3.51-fold basal release) and a reduction of 43% with respect to Munc13-1$^{H567K/+}$ mice (Fig. 5*A*). The results corroborate the above in vivo results (Fig. 4*B*). Diacylglycerol (DAG) and phorbol esters are known to potentiate insulin secretion, mainly by increasing the size of insulin granules pools, and by accelerating the mobilization of insulin granules for subsequent priming and release (2). We therefore assessed the potentiation of GSIS by PMA, a phorbol ester that binds Munc13-1 at the same site as DAG (18–20). Indeed, 200 nmol/l PMA stimulation potentiated 16 mmol/l GSIS in Munc13-1$^{+/-}$ islets (Fig. 5*B*), indicating that the residual Munc13-1 proteins in the islets of heterozygous Munc13-1$^{+/-}$ mice are functional. Nevertheless, PMA potentiation of GSIS relative to 16 mmol/l GSIS was greatly suppressed by 49.2% in Munc13-1$^{+/-}$ islets (2.42-fold) with respect to Munc13-1$^{+/+}$ islets (4.76-fold) (Fig. 5*B*). These results indicate that the binding of PMA to the residual Munc13-1 proteins in the Munc13-1$^{+/-}$ islets, but not PKC, which is not deficient in these transgenic mice (Fig. 1*B*), primarily accounts for enhancement of insulin secretion by PMA.

For the Munc13-1$^{H567K/+}$ islets, GSIS was mildly but not significantly reduced when compared with Munc13-1$^{+/+}$ mice islets (Fig. 5*A*), corroborating the above in vivo insulin secretion data (Fig. 4*B*). The potentiation (secretion above that evoked by 16 mmol/l glucose alone) of insulin secretion by 200 nmol/l PMA was nonetheless modestly reduced but less so than in Munc13-1$^{+/-}$ islets (Fig. 5*B*). The reason for the better GSIS response of the Munc13-1$^{H567K/+}$ islets compared with the Munc13-1$^{+/-}$ islets is that the Munc13-1 H567K DAG-binding site mutant protein, although defective in its ability to translocate to the plasma membrane, contains an intact priming domain that is distinct from the DAG-binding site (28,29) and therefore is able to retain some priming function (19,22). Nonetheless, these results show that an intact C1 PMA/DAG-binding domain of Munc13-1 is required for a fully efficacious potentiation of GSIS by PMA.

The differences in GSIS between the groups suggest the possibility of compensatory mechanisms such as increased islet mass (30) or increased (pro)-insulin biosynthesis. Total insulin contents were comparable between

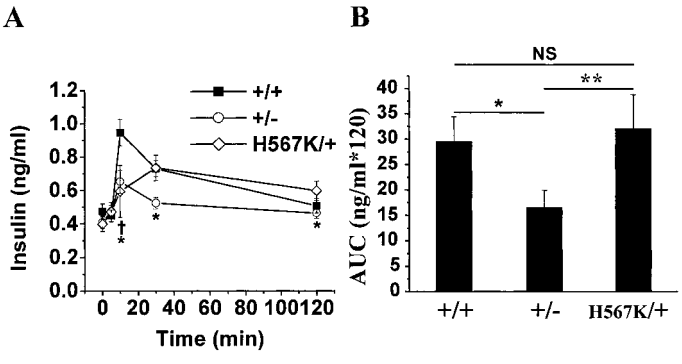

FIG. 4. In vivo insulin secretory response to a glucose challenge is reduced in Munc13-1$^{+/-}$ mice but not in Munc13-1$^{H567K/+}$ mice. *A*: A single intraperitoneal glucose (1 g/kg body wt) challenge test was performed on 12- to 16-h–fasted Munc13-1$^{+/+}$, Munc13-1$^{+/-}$, and Munc13-1$^{H567K/+}$ mice and serum insulin levels measured as described under RESEARCH DESIGN AND METHODS. A mean ± SE of ~10 animals per group was shown. *P < 0.05 for Munc13-1$^{+/-}$ vs. Munc13-1$^{+/+}$ at t = 10, 30, and 120 min. †P < 0.05 for Munc13-1$^{H567K/+}$ vs. Munc13-1$^{+/+}$ at t = 10 min. **P < 0.05 for Munc13-1$^{+/-}$ vs. Munc13-1$^{H567K/+}$ at t = 120 min. *B*: A mean ± SE of areas under the curve of serum insulin levels during the IPGTT are shown. *P < 0.05 for Munc13-1$^{+/-}$ vs. Munc13-1$^{+/+}$. **P < 0.05 for Munc13-1$^{+/-}$ vs. Munc13-1$^{H567K/+}$.

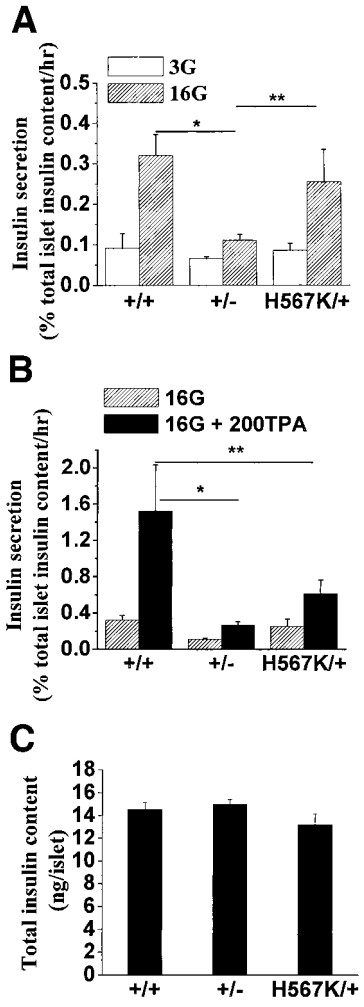

FIG. 5. Assessment of insulin secretion in response to glucose and PMA in islets of Munc13-1$^{+/+}$, Munc13-1$^{+/-}$, and Munc13-1$^{H567K/+}$ mice. Groups of 30 islets from Munc13-1$^{+/+}$, Munc13-1$^{+/-}$, and Munc13-1$^{H567K/+}$ mice were incubated for 1 h at 3 mmol/l glucose followed by 1 h at 16 mmol/l glucose without (*A*) or with (*B*) 200 nmol/l PMA. Data are means ± SE of 20 determinations in five separate experiments. Insulin released was normalized to total insulin content. *P < 0.05 for Munc13-1$^{+/-}$ vs. Munc13-1$^{+/+}$. **P < 0.05 for Munc13-1$^{+/-}$ vs. Munc13-1$^{H567K/+}$. *C*: Islet insulin contents in Munc13-1$^{+/+}$, Munc13-1$^{+/-}$, and Munc13-1$^{H567K/+}$ mice. Means ± SE (n = 15–20 per group).

isolated islets of the three groups (Fig. 5*C*), which argues against a difference in insulin biosynthesis as a compensatory mechanism explaining the differences in insulin secretory responses in these mice.

Munc13-1$^{+/-}$ and Munc13-1$^{H567K/+}$ islet β-cells exhibit distinct impairment in priming and mobilization of insulin granule pools. To examine the direct contribution of islet β-cell insulin secretory defect in the Munc13-1$^{+/-}$ mice, we employed patch-clamp membrane capacitance (C_m) measurements of single-islet β-cells. We used a protocol of eight serial depolarizing pulses where the first two pulses would release the initially primed RRP of insulin granules, and subsequent pulses would cause the mobilization of granules from the reserve pool(s) to refill the releasable pool (31,32). Compared with Munc13-1$^{+/+}$ β-cells, C_m increases in Munc13-1$^{+/-}$ β-cells were significantly reduced at every depolarizing pulse, with a 62% reduction of RRP size (6.45 ± 0.69 vs. 2.42 ± 0.36 fF/pF at 2nd pulse, $P < 0.05$) and a 36% reduction of granules refilling/mobilization ($\Delta Cm_{3rd\text{-}8thpulse}$) (7.65 ± 0.73 vs. 4.86 ± 0.33 fF/pF, $P < 0.05$) (Fig. 6*A* and *C*). This result is consistent with the result of the whole-islet secretion assays (Fig. 5). PMA pretreatment enhanced insulin exocytosis in Munc13-1$^{+/+}$ β-cells by threefold compared with no PMA pretreatment (39.5 ± 3.18 vs. 13.23 ± 0.72 fF/pF at 8th pulse, $P < 0.05$), where the RRP size was 15.54 ± 2.03 fF/pF at 2nd pulse, and $\Delta Cm_{3rd\text{-}8thpulse}$ was 24.56 ± 2.80 fF/pF (Fig. 6*B* and *D*). In contrast, PMA potentiation of insulin exocytosis in Munc13-1$^{+/-}$ β-cells was reduced to only twofold (17.33 ± 1.28 vs. 7.46 ± 0.50 fF/pF at 8th pulse), where the RRP size is 7.18 ± 0.73 fF/pF at 2nd pulse, and $\Delta Cm_{3rd\text{-}8thpulse}$ was 11.98 ± 0.80 fF/pF (Fig. 6*B* and *D*). In absolute terms, the cumulative increase in C_m was reduced even more (by 56%) in Munc13-1$^{+/-}$ β-cells compared with Munc13-1$^{+/+}$ β-cells (17.33 ± 1.28 vs. 39.5 ± 3.18 fF/pF), including a 54% reduction ($P < 0.05$) in the RRP ($\Delta Cm_{1st–2nd\ pulse}$) and 51% reduction ($P < 0.05$) in the rate of granules pool mobilization ($\Delta Cm_{3rd–8th\ pulse}$). These results suggest that a deficiency in Munc13-1 expression greatly impairs Ca^{2+}-evoked and PMA-potentiated exocytosis, specifically by reducing the size of the primed RRP and impairing the rate of granules refilling/mobilization.

As for Munc13-1$^{H567K/+}$ β-cells, there is also a reduction in the initial size of the primed RRP compared with Munc13-1$^{+/+}$ β-cells (3.83 ± 0.94 v.s. 6.45 ± 0.69 fF/pF at 2nd pulse, $P < 0.05$) (Fig. 6*A* and *C*). However, the subsequent pulses evoked C_m increases ($\Delta Cm_{3rd–8th\ pulse}$) in Munc13-1$^{H567K/+}$ β-cells comparable to those in Munc13-1$^{+/+}$ β-cells, indicating that the rate of refilling of the RRP was not impaired (8.49 ± 1.21 vs. 7.65 ± 0.73 fF/pF, P = 0.56) (Fig. 6*A* and *C*). These results are consistent with the in vivo results showing an impaired first-phase but not second-phase secretion in Munc13-1$^{H567K/+}$ mice (Fig. 4). This deficiency of Munc13-1 binding to phorbol ester/DAG caused only a mild impairment of priming of granules in RRP as to cause a reduction of the initial size of the RRP but seemed to not affect the refilling of RRP under these stimulatory conditions. However, upon increased demand by PMA pretreatment, the priming deficiency became accentuated by the deficiency of Munc13-1 binding to phorbol ester/DAG, revealing not only a reduction in the initial size of the RRP (by 27%) compared with Munc13-1$^{+/+}$ β-cells (11.42 ± 1.07 vs. 15.54 ± 2.03 fF/pF at 2nd pulse, $P < 0.05$) but, remarkably, also a similar reduction (by 36%) in the refilling ($\Delta Cm_{3rd–8th\ pulse}$) of the RRP compared with Munc13-1$^{+/+}$ β-cells (15.76 ± 0.88 vs. 24.56 ± 2.80 fF/pF, $P < 0.05$) (Fig. 6*B* and *D*).

Ca_V and K_V currents are unaltered in Munc13-1$^{+/-}$ and Munc13-1$^{H567K/+}$ islet β-cells. The impaired insulin exocytosis phenotype described above could be caused by perturbations in essentially any step of the insulin vesicle cycle and in particular the Ca^{2+}-triggering step (33). Ca^{2+} plays a role not only as a trigger for exocytosis but also in the priming of insulin vesicles (2). It is thus possible that Munc13-1 deficiency could alter Ca^{2+} release pathways directly or indirectly via its actions on syntaxin 1A, the latter having direct effects on Ca^{2+} channels in pancreatic β-cells (34,35). We therefore examined possible alterations in the voltage-gated Ca^{2+} channel activity by the Munc13-1 deficiency. In both Munc13-1$^{+/-}$ and Munc13-1$^{H567K/+}$ β-cells, we observed no significant changes in either Ca_V current amplitudes (Figs. 7*A* and *B*) or channel gating (steady-state inactivation; data not shown). The waveform of action potentials is shaped by the activity of voltage-gated K^+ channels in the pancreatic β-cells, the majority of

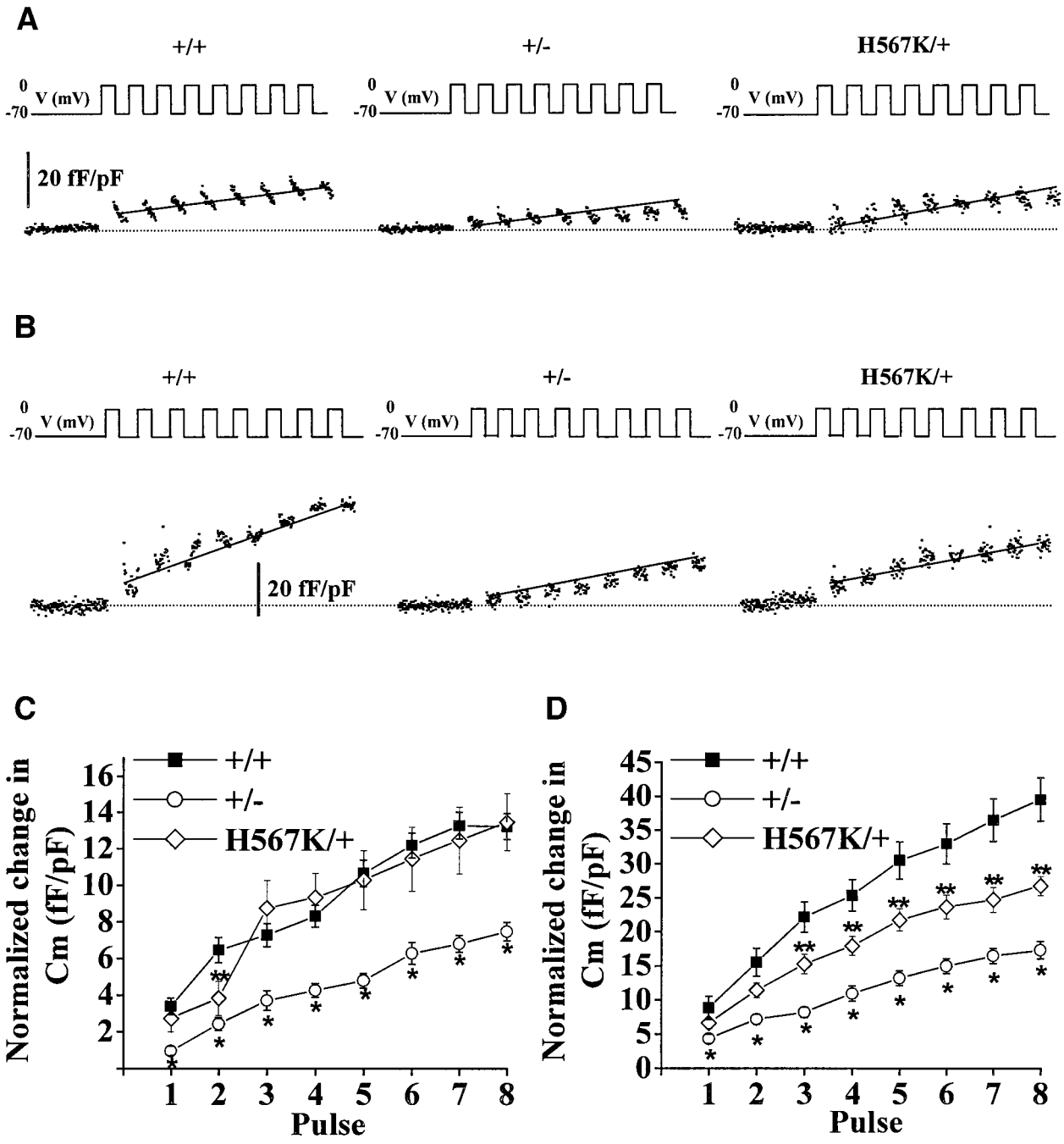

FIG. 6. Exocytosis in single islet β-cells of Munc13-1$^{+/+}$, Munc13-1$^{+/-}$, and Munc13-1$^{H567K/+}$ mice. Changes in cell C_m (ΔC_m) were measured from single β-cells using a train of eight depolarizing pulses (500 ms in duration) from −70 to 0 mV. *A* and *B* show representative recordings of ΔC_m normalized to basal cell C_m (fF/pF) from a Munc13-1$^{+/+}$ β-cell, a Munc13-1$^{+/-}$ β-cell, and a Munc13-1$^{H567K/+}$ β-cell evoked by depolarizations alone (*A*) and after pretreatment with 200 nmol/l PMA (*B*). *C* and *D* show the corresponding summaries of the changes in ΔC_m normalized to basal cell C_m (fF/pF) from Munc13-1$^{+/+}$, Munc13-1$^{+/-}$, and Munc13-1$^{H567K/+}$ β-cells evoked by depolarizations alone (n = 12–15 cells) (*C*) and after pretreatment with 200 nmol/l PMA (n = 19–23 cells) (*D*). Points represent the mean ± SE. *$P < 0.05$ for Munc13-1$^{+/-}$ vs. Munc13-1$^{+/+}$; **$P < 0.05$ for Munc13-1$^{H567K/+}$ vs. Munc13-1$^{+/+}$.

which are the delayed rectifier, Kv2.1, whose activity is modulated by syntaxin 1A (36,37). However, we observed no significant changes in K_V current amplitudes in the Munc13-1 mutant mice islet β-cells (Figs. 7*C* and *D*).

DISCUSSION

Munc13-1 is an essential secretory vesicle–priming protein (10,13,14) that facilitates the formation of a stable SNARE complex by directly interacting with (38) and switching syntaxin 1A from a "closed" to an "open" conformation (8,16) and thus allowing syntaxin 1A to bind the cognate SNARE proteins (39). As in neurons, we previously provided evidence that Munc13-1 in pancreatic β-cells is the major phorbol ester/DAG receptor involved in phorbol ester/DAG-induced potentiation of insulin exocytosis (20). In this report, we directly show that Munc13-1 reduction alone is sufficient to cause abnormal GSIS and glucose homeostasis mimicking diabetes. The dramatic phenotype of impaired synaptic transmitter release in Munc13-1 knockout mice is a consequence of a reduced primed and

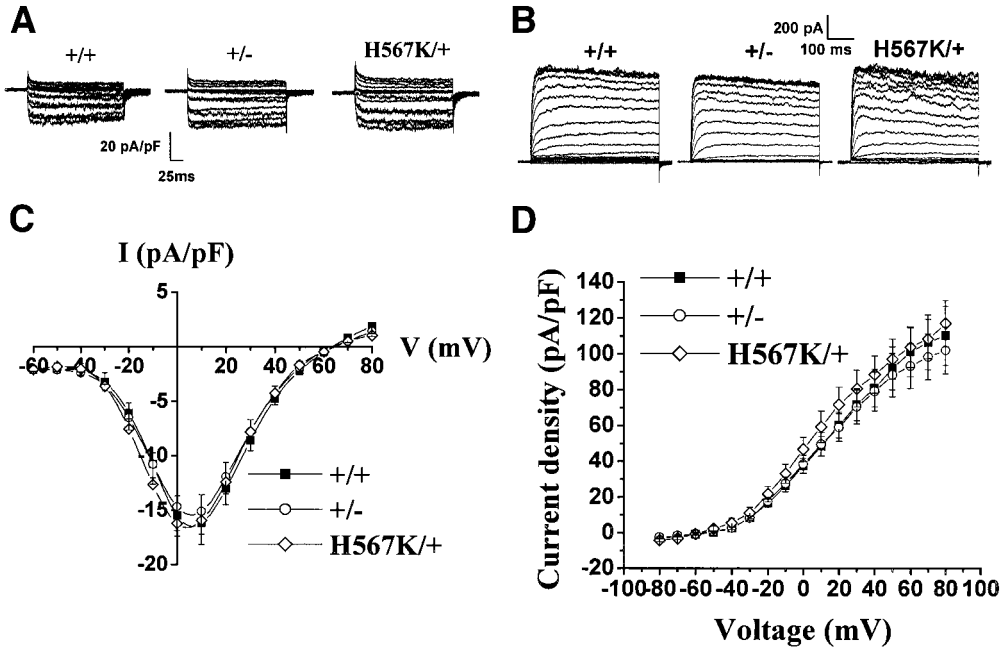

FIG. 7. Ca_V and K_V current amplitudes in isolated β-cells from Munc13-$1^{+/+}$, Munc13-$1^{+/-}$, and Munc13-$1^{H567K/+}$ mice. *A*: Representative Ca_V currents recorded in the whole-cell mode using 20 mmol/l $BaCl_2$ in the bath solution and 20 mmol/l tetraethylammonium inside the patch electrode and outside the cell to block K_V currents. Cells were held at −80 mV, and currents were elicited by step depolarizations from −60 to +80 mV. *B*: Current-voltage relationship of Ca_V channels. Values are means ± SE (n = 10–15 cells). *C*: Representative whole-cell recordings of K_V currents. Cells were held at −70 mV, and currents were elicited by step depolarizations from −80 to +80 mV. *D*: Current-voltage relationship of K_V channels. Values are means ± SE (n = 10–15 cells).

RRP size (13,18,19). For neurotransmitter release, total Munc13-1 deletion is required to abrogate priming (13,19). In the present study, a deletion of one *Munc13-1* allele resulting in the depletion in islet tissues of Munc13-1 to levels mimicking those seen in diabetic islets (20,21) was sufficient to induce an insulin secretory defect. This occurred with no detectable effects on the levels of Munc13-1–interacting exocytic proteins, which was observed with the complete Munc13-1 deletion (13). These observations in brain and islet tissues may be explained by a functional redundancy of Munc13 isoforms in neurons to compensate for the Munc13-1 deficiency (19) but which may not be present or abundant in pancreatic islets.

In diabetes, the first phase of insulin secretion is abrogated, and the subsequent sustained second-phase response is blunted. As in neurons, the primed RRP granules pool accounting for the first phase of insulin release requires the formation of the SNARE ternary complex (2). The reduced levels of Munc13-1 in type 2 diabetes rat models (20) and diabetic human islets (21) could therefore be a major contributing factor to the reduced first phase of insulin secretion as observed with the Munc13-$1^{+/-}$ mice. The second phase of release is accounted for by additional insulin granules being recruited to refill the RPP (4). We show that the second phase of insulin release was also severely reduced in the Munc13-$1^{+/-}$ mice, indicating the important role of Munc13-1 in both phases of insulin secretion. Indeed, our C_m studies support this thinking, demonstrating that both the initial size of primed RRP and subsequent mobilization of granules from the reserve pool to the RRP are reduced in the Munc13-$1^{+/-}$ β-cells (Fig. 6*A* and *C*).

A surprising result is that the Munc13-$1^{H567K/+}$ mice exhibited only a reduced first phase of insulin release (Fig. 4*A*) but a normal second phase, which was not sufficient to induce an abnormal glucose tolerance. Consistently, the C_m study showed only a reduced sized of the primed RRP but normal mobilization of the reserve pool (Fig. 6*A* and *C*). The normal glucose tolerance was not due to a compensatory increase in islet mass or insulin biosynthesis since total insulin content per islet (Fig. 5*C*) remained unaltered. It could be attributed to possible compensatory mechanisms such as the actions of the other islet secretory cells, which could also be regulated by Munc13-1 priming actions, including a reduction of paracrine inhibition by somatostatin released by islet δ cells or a reduction of counterregulatory neuronal and endocrine modulation. Nonetheless, when additional demand by PMA potentiation was imposed on the Munc13-$1^{H567K/+}$ β-cells, a deficiency in mobilization of the reserve pool to the RRP was also observed, albeit less severe than in Munc13-$1^{+/-}$ β-cells (Fig. 6*B* and *D*). This is corroborated by reduced PMA potentiation of GSIS in Munc13-$1^{H567K/+}$ islets (Fig. 5*B*). Although our C_m protocol would be considered to be supraphysiologic stimulation, high and sustained glycemic demand on the islets certainly occur in diabetes and would have a similar imposition on the deficient islet Munc13-1 levels (20,21). Taken together, these results suggest that Munc13-1 is a major phorbol ester and DAG substrate in the islet β-cell to prime insulin granules within the RRP and which determines the initial size of the RRP and the efficiency of mobilization of granules into the RRP.

These results also complement our previous studies (20,40) showing that an intact C1 domain is essential for soluble Munc13-1 translocation to the plasma membrane in response to phorbol ester and DAG activation. Translocation of soluble Munc13-1 to the plasma membrane is thought to create additional priming sites, particularly when the membrane-bound Munc13-1 in the presynaptic active zone is functionally saturated (19). The Munc13-$1^{H567K/+}$ mice islet β-cells secreted more insulin than Munc13-$1^{+/-}$ mice, which we attribute to the fact that the Munc13-1^{H567K} mutant variant, although defective in its C1 domain, still has some capability of transducing its priming action since the priming domain was recently localized to a α-helical domain in the COOH-terminus (28,29,41). Consistently, overexpression of Munc13-1^{H567K}–EGFP (enhanced green fluorescent protein) in insulinoma cells (20) and adrenal chromaffin cells (40) potentiated exocytosis over vector-transfected controls but less than overexpression of the wild-type Munc13-1 protein.

In Munc13-$1^{H567K/+}$ mice, the normal second phase of

release by GSIS (Fig. 4*A*) and normal mobilization of insulin granules into the RRP (Fig. 6*A* and *C*) indicate that additional cell signals or molecules in islet β-cells may come into play during the second phase, which are capable of compensating for the milder Munc13-1 dysfunction in the Munc13-$1^{H567K/+}$ islets, but become less efficient when Munc13-1 levels are reduced as in the Munc13-$1^{+/-}$ islets (and in diabetes [20,21]). The major DAG substrates include many PKC isoforms, particularly cPKC (PKC-α) and nPKC (PKC-ϵ), which were unchanged in the islets of the three mice (Fig. 1*B*). Nonetheless, this does not preclude the possibility that normal levels of these (25,27,42) as well as other PKCs, such as cPKC-βII and nPKC-δ (26,43,44), may also serve as DAG receptors capable of being activated, undergo cellular translocation, and exert additional and independent priming actions on insulin exocytosis. More studies performed on these mice islets will be required to see if these PKCs act either sequentially to Munc13-1 or in parallel, perhaps in a manner capable of bypassing the Munc13-1 deficiency.

L-Type voltage-gated calcium channels in pancreatic β-cells provide the primary source of Ca^{2+} entry into the pancreatic β-cells to trigger insulin exocytosis (3). However, the density of the channels in pancreatic β-cells is considerably lower than that in synapses of nerve cells and in adrenal chromaffin cells (3,45). It was suggested that a subset of insulin granules in the RRP is situated in the immediate vicinity of the L-type Ca^{2+} channels to allow efficient triggering of exocytosis by Ca^{2+} entry (3). This was proposed to be caused by tethering of the Ca^{2+} channels to the subset of granules within the RRP (45). Ca^{2+} channels as well as the major membrane-repolarizing K^+ channel in islet β-cells, Kv2.1, are also profoundly influenced by distinct conformations of syntaxin 1A (36,37,46). It is therefore possible that a Munc13-1 deficiency could indirectly influence Ca^{2+} or Kv2.1 channel gating by actions on syntaxin 1A. However, we observed here that Munc13-1 deficiency did not alter voltage-gated Ca^{2+} or Kv channels activity. Moreover, calcium ionophores cannot bypass the Munc13-1 mutant phenotype in hippocampal neurons, indicating that Munc13-1 deficiency does not interfere with Ca^{2+} triggering of transmitter release (13).

In summary, our study shows that a 60% reduction of Munc13-1 expression or function is sufficient to cause defects in both first and second phases of insulin release, more so than in the neuronal synapse, and is in fact sufficient to cause abnormalities in glucose homeostasis mimicking type 2 diabetes. Since the RRP in the islet β-cells is much smaller than in neurons and chromaffin cells (47) and because islet β-cells express only low levels of Munc13-1 proteins, a smaller perturbation of Munc13-1 expression or function would be expected to cause defects in insulin exocytosis. In fact, pancreatic islet Munc13-1 levels in type 2 diabetic rodents (20) and humans (21) are reduced to levels similar to those observed in the Munc13-1–deficient mice studied. Thus, the results provide direct evidence that Munc13-1 is an important player in the transduction mechanism of the β-cell in response to glucose. It can be hypothesized that glucose-induced increases in DAG following inhibition of fat oxidation by malonyl CoA (48) or enhanced lipolysis (49) promote insulin exocytosis via the DAG receptor Munc13-1. As such, Munc13-1 may be the late-signaling effector of fuel-induced insulin secretion. The possibility should be considered that upregulation of Munc13 levels or priming function may be therapeutically effective in restoring the defective insulin secretion in diabetes.

ACKNOWLEDGMENTS

This work was supported by grants to H.Y.G. from the Canadian Institutes of Health Research (CIHR; MOP64465) and equipment grants from CIHR (MMA 66939) and the University of Toronto Banting and Best Diabetes Center (BBDC). E.P.K. is supported by a Canada Graduate Scholarships Doctoral Award from CIHR (CGD 76317) and the University of Toronto-BBDC (Tamarack Studentship Award). N.B. is supported by the German Research Foundation (SFB406/A1).

REFERENCES

1. Rorsman P, Renstrom E: Insulin granule dynamics in pancreatic beta cells. *Diabetologia* 46:1029–1045, 2003
2. Straub SG, Sharp GW: Glucose-stimulated signaling pathways in biphasic insulin secretion. *Diabetes Metab Res Rev* 18:451–463, 2002
3. Barg S, Eliasson L, Renstrom E, Rorsman P: A subset of 50 secretory granules in close contact with L-type Ca2+ channels accounts for first-phase insulin secretion in mouse beta-cells. *Diabetes* 51 (Suppl. 1):S74–S82, 2002
4. Olofsson CS, Gopel SO, Barg S, Galvanovskis J, Ma X, Salehi A, Rorsman P, Eliasson L: Fast insulin secretion reflects exocytosis of docked granules in mouse pancreatic B-cells. *Pflugers Arch* 444:43–51, 2002
5. Sudhof TC: The synaptic vesicle cycle: a cascade of protein-protein interactions. *Nature* 375:645–653, 1995
6. Wheeler MB, Sheu L, Ghai M, Bouquillon A, Grondin G, Weller U, Beaudoin AR, Bennett MK, Trimble WS, Gaisano HY: Characterization of SNARE protein expression in beta cell lines and pancreatic islets. *Endocrinology* 137:1340–1348, 1996
7. Weber T, Zemelman BV, McNew JA, Westermann B, Gmachl M, Parlati F, Sollner TH, Rothman JE: SNAREpins: minimal machinery for membrane fusion. *Cell* 92:759–772, 1998
8. Brose N, Rosenmund C, Rettig J: Regulation of transmitter release by Unc-13 and its homologues. *Curr Opin Neurobiol* 10:303–311, 2000
9. Maruyama IN, Brenner S: A phorbol ester/diacylglycerol-binding protein encoded by the unc-13 gene of *Caenorhabditis elegans*. *Proc Natl Acad Sci U S A* 88:5729–5733, 1991
10. Aravamudan B, Fergestad T, Davis WS, Rodesch CK, Broadie K: Drosophila UNC-13 is essential for synaptic transmission. *Nat Neurosci* 2:965–971, 1999
11. Augustin I, Betz A, Herrmann C, Jo T, Brose N: Differential expression of two novel Munc13 proteins in rat brain. *Biochem J* 337:363–371, 1999
12. Brose N, Hofmann K, Hata Y, Sudhof TC: Mammalian homologues of *Caenorhabditis elegans* unc-13 gene define novel family of C2-domain proteins. *J Biol Chem* 270:25273–25280, 1995
13. Augustin I, Rosenmund C, Sudhof TC, Brose N: Munc13-1 is essential for fusion competence of glutamatergic synaptic vesicles. *Nature* 400:457–461, 1999
14. Richmond JE, Davis WS, Jorgensen EM: UNC-13 is required for synaptic vesicle fusion in *C. elegans*. *Nat Neurosci* 2:959–964, 1999
15. Varoqueaux F, Sigler A, Rhee JS, Brose N, Enk C, Reim K, Rosenmund C: Total arrest of spontaneous and evoked synaptic transmission but normal synaptogenesis in the absence of Munc13-mediated vesicle priming. *Proc Natl Acad Sci U S A* 99:9037–9042, 2002
16. Richmond JE, Weimer RM, Jorgensen EM: An open form of syntaxin bypasses the requirement for UNC-13 in vesicle priming. *Nature* 412:338–341, 2001
17. Koch H, Hofmann K, Brose N: Definition of Munc13-homology-domains and characterization of a novel ubiquitously expressed Munc13 isoform. *Biochem J* 349:247–253, 2000
18. Betz A, Ashery U, Rickmann M, Augustin I, Neher E, Sudhof TC, Rettig J, Brose N: Munc13-1 is a presynaptic phorbol ester receptor that enhances neurotransmitter release. *Neuron* 21:123–136, 1998
19. Rhee JS, Betz A, Pyott S, Reim K, Varoqueaux F, Augustin I, Hesse D, Sudhof TC, Takahashi M, Rosenmund C, Brose N: Beta phorbol ester- and diacylglycerol-induced augmentation of transmitter release is mediated by Munc13s and not by PKCs. *Cell* 108:121–133, 2002
20. Sheu L, Pasyk EA, Ji J, Huang X, Gao X, Varoqueaux F, Brose N, Gaisano HY: Regulation of insulin exocytosis by Munc13-1. *J Biol Chem* 278:27556–27563, 2003

21. Ostenson CG, Gaisano H, Sheu L, Tibell A, Bartfai T: Impaired gene and protein expression of exocytotic soluble *N*-ethylmaleimide attachment protein receptor complex proteins in pancreatic islets of type 2 diabetic patients. *Diabetes* 55:435–440, 2006
22. Rosenmund C, Sigler A, Augustin I, Reim K, Brose N, Rhee JS: Differential control of vesicle priming and short-term plasticity by Munc13 isoforms. *Neuron* 33:411–424, 2002
23. Gopel S, Kanno T, Barg S, Galvanovskis J, Rorsman P: Voltage-gated and resting membrane currents recorded from B-cells in intact mouse pancreatic islets. *J Physiol* 521:717–728, 1999
24. Lindau M, Neher E: Patch-clamp techniques for time-resolved capacitance measurements in single cells. *Pflugers Arch* 411:137–146, 1988
25. Mendez C, Bertorello A: Rapid association of protein kinase C-epsilon with insulin granules is essential for insulin exocytosis. *J Biol Chem* 2003
26. Yaney GC, Fairbanks JM, Deeney JT, Korchak HM, Tornheim K, Corkey BE: Potentiation of insulin secretion by phorbol esters is mediated by PKC-alpha and nPKC isoforms. *Am J Physiol Endocrinol Metab* 283:E880–E888, 2002
27. Zaitsev SV, Efendic S, Arkhammar P, Bertorello AM, Berggren PO: Dissociation between changes in cytoplasmic free Ca2+ concentration and insulin secretion as evidenced from measurements in mouse single pancreatic islets. *Proc Natl Acad Sci U S A* 92:9712–9716, 1995
28. Basu J, Shen N, Dulubova I, Lu J, Guan R, Guryev O, Grishin NV, Rosenmund C, Rizo J: A minimal domain responsible for Munc13 activity. *Nat Struct Mol Biol* 12:1017–1018, 2005
29. Stevens DR, Wu ZX, Matti U, Junge HJ, Schirra C, Becherer U, Wojcik SM, Brose N, Rettig J: Identification of the minimal protein domain required for priming activity of munc13-1. *Curr Biol* 15:2243–2248, 2005
30. Leroux L, Desbois P, Lamotte L, Duvillie B, Cordonnier N, Jackerott M, Jami J, Bucchini D, Joshi RL: Compensatory responses in mice carrying a null mutation for Ins1 or Ins2. *Diabetes* 50 (Suppl. 1):S150–S153, 2001
31. Gillis KD, Mossner R, Neher E: Protein kinase C enhances exocytosis from chromaffin cells by increasing the size of the readily releasable pool of secretory granules. *Neuron* 16:1209–1220, 1996
32. Kanno T, Ma X, Barg S, Eliasson L, Galvanovskis J, Gopel S, Larsson M, Renstrom E, Rorsman P: Large dense-core vesicle exocytosis in pancreatic beta-cells monitored by capacitance measurements. *Methods* 33:302–311, 2004
33. Gerber SH, Rizo J, Sudhof TC: Role of electrostatic and hydrophobic interactions in Ca^{2+}-dependent phospholipid binding by the C(2)A-domain from synaptotagmin I. *Diabetes* 51 (Suppl. 1):S12–S18, 2002
34. Lam PP, Leung YM, Sheu L, Ellis J, Tsushima RG, Osborne LR, Gaisano HY: Transgenic mouse overexpressing syntaxin-1A as a diabetes model. *Diabetes* 54:2744–2754, 2005
35. Wiser O, Trus M, Hernandez A, Renstrom E, Barg S, Rorsman P, Atlas D: The voltage sensitive Lc-type Ca2+ channel is functionally coupled to the exocytotic machinery. *Proc Natl Acad Sci U S A* 96:248–253, 1999
36. Leung YM, Kang Y, Gao X, Xia F, Xie H, Sheu L, Tsuk S, Lotan I, Tsushima RG, Gaisano HY: Syntaxin 1A binds to the cytoplasmic C terminus of Kv2.1 to regulate channel gating and trafficking. *J Biol Chem* 278:17532–17538, 2003
37. Leung YM, Kang Y, Xia F, Sheu L, Gao X, Xie H, Tsushima RG, Gaisano HY: Open form of syntaxin-1A is a more potent inhibitor than wild-type syntaxin-1A of Kv2.1 channels. *Biochem J* 387:195–202, 2005
38. Betz A, Okamoto M, Benseler F, Brose N: Direct interaction of the rat unc-13 homologue Munc13-1 with the N terminus of syntaxin. *J Biol Chem* 272:2520–2526, 1997
39. Dulubova I, Sugita S, Hill S, Hosaka M, Fernandez I, Sudhof TC, Rizo J: A conformational switch in syntaxin during exocytosis: role of munc18. *EMBO J* 18:4372–4382, 1999
40. Ashery U, Varoqueaux F, Voets T, Betz A, Thakur P, Koch H, Neher E, Brose N, Rettig J: Munc13-1 acts as a priming factor for large dense-core vesicles in bovine chromaffin cells. *EMBO J* 19:3586–3596, 2000
41. Madison JM, Nurrish S, Kaplan JM: UNC-13 interaction with syntaxin is required for synaptic transmission. *Curr Biol* 15:2236–2242, 2005
42. Deeney JT, Cunningham BA, Chheda S, Bokvist K, Juntti-Berggren L, Lam K, Korchak HM, Corkey BE, Berggren PO: Reversible Ca2+-dependent translocation of protein kinase C and glucose-induced insulin release. *J Biol Chem* 271:18154–18160, 1996
43. Wan QF, Dong Y, Yang H, Lou X, Ding J, Xu T: Protein kinase activation increases insulin secretion by sensitizing the secretory machinery to Ca2+. *J Gen Physiol* 124:653–662, 2004
44. Yang Y, Gillis KD: A highly Ca2+-sensitive pool of granules is regulated by glucose and protein kinases in insulin-secreting INS-1 cells. *J Gen Physiol* 124:641–651, 2004
45. Barg S, Ma X, Eliasson L, Galvanovskis J, Gopel SO, Obermuller S, Platzer J, Renstrom E, Trus M, Atlas D, Striessnig J, Rorsman P: Fast exocytosis with few Ca(2+) channels in insulin-secreting mouse pancreatic B cells. *Biophys J* 81:3308–3323, 2001
46. Jarvis SE, Barr W, Feng ZP, Hamid J, Zamponi GW: Molecular determinants of syntaxin 1 modulation of N-type calcium channels. *J Biol Chem* 277:44399–44407, 2002
47. Eliasson L, Renstrom E, Ding WG, Proks P, Rorsman P: Rapid AT: P-dependent priming of secretory granules precedes Ca(2+)-induced exocytosis in mouse pancreatic B-cells. *J Physiol* 503:399–412, 1997
48. Prentki M, Vischer S, Glennon MC, Regazzi R, Deeney JT, Corkey BE: Malonyl-CoA and long chain acyl-CoA esters as metabolic coupling factors in nutrient-induced insulin secretion. *J Biol Chem* 267:5802–5810, 1992
49. Peyot ML, Nolan CJ, Soni K, Joly E, Lussier R, Corkey BE, Wang SP, Mitchell GA, Prentki M: Hormone-sensitive lipase has a role in lipid signaling for insulin secretion but is nonessential for the incretin action of glucagon-like peptide 1. *Diabetes* 53:1733–1742, 2004